RAA 2016 Vol. **16** No. **8**, 118 (8pp) doi: 10.1088/1674–4527/16/8/118
http://www.raa-journal.org *http://iopscience.iop.org/raa*

Research in Astronomy and Astrophysics

The core dominance parameter and *Fermi* detection of extragalactic radio sources

Zhen-Kuo Liu[1], Zhong-Zu Wu[1] and Min-Feng Gu[2]

[1] College of Science, Guizhou University, Guiyang 550025, China; *zzwu08@gmail.com*
[2] Key Laboratory for Research in Galaxies and Cosmology, Shanghai Astronomical Observatory, Chinese Academy of Sciences, Shanghai 200030, China

Received 2015 December 18; accepted 2016 March 4

Abstract By cross-correlating an archive sample of 542 extragalactic radio sources with the *Fermi*-LAT Third Source Catalog (3FGL), we have compiled a sample of 80 γ-ray sources and 462 non-*Fermi* sources with available core dominance parameter ($R_{\rm CD}$), and core and extended radio luminosity; all the parameters are directly measured or derived from available data in the literature. We found that $R_{\rm CD}$ has significant correlations with radio core luminosity, γ-ray luminosity and γ-ray flux; the *Fermi* sources have on average higher $R_{\rm CD}$ than non-*Fermi* sources. These results indicate that the *Fermi* sources should be more compact, and the beaming effect should play a crucial role in the detection of γ-ray emission. Moreover, our results also show *Fermi* sources have systematically larger radio flux than non-*Fermi* sources at fixed $R_{\rm CD}$, indicating larger intrinsic radio flux in *Fermi* sources. These results show a strong connection between radio and γ-ray flux for the present sample and indicate that the non-*Fermi* sources are likely due to the low beaming effect, and/or the low intrinsic γ-ray flux. This supports a scenario that has been published in the literature: a co-spatial origin of the activity for the radio and γ-ray emission, suggesting that the origin of the seed photons for the high-energy γ-ray emission is within the jet.

Key words: BL Lacertae objects: general — galaxies: active — quasars: general — galaxies: general — gamma-rays: general

1 INTRODUCTION

Blazars are the most extreme active galactic nuclei (AGNs) with characteristic properties such as large and variable polarization, apparent superluminal motion, flat or inverted radio spectra, and a broad continuum from radio through γ-rays (e.g., Urry & Padovani 1995). Because of the launch of the *Fermi* satellite, the whole γ-ray sky has been scanned once approximately every three hours since July of 2008 by the onboard Large Area Telescope (LAT) (e.g., Atwood et al. 2009). The third LAT AGN catalog (Ackermann et al. 2015) and *Fermi*-LAT Third Source Catalog (3FGL) (Acero et al. 2015) showed that among all the *Fermi* detected AGNs (FAGNs), nearly all of them are blazars. However, it should be noted that there are far more blazars and other types of AGNs that are not detected by *Fermi*.

The differences between FAGNs and non-*Fermi* AGNs (NFAGNs) have been addressed in the literature. Piner et al. (2012) showed that sources detected with *Fermi* have higher apparent speeds than those sources not detected with *Fermi*. Pushkarev & Kovalev (2012) found that the FAGNs have higher brightness temperature and VLBI core flux densities. Linford et al. (2012) showed that Fermi detected BL Lacs (FBLs) have longer jets and are polarized more often. Wu et al. (2014) selected a sample of 100 FBLs and 70 non-*Fermi* BL Lacs (NFBLs) and found that the Doppler factor and intrinsic radio flux are on average larger in FBLs than in NFBLs. Based on a large sample of blazars, Xiong et al. (2015) found that there are significant differences between *Fermi* blazars and non-*Fermi* blazars for differing black hole mass, jet kinetic power from "cavity" power, and broad-line luminosity.

By now, Doppler boosting is believed to be one important answer for the question "why are some sources γ-ray loud and others are γ-ray quiet" (Lister et al. 2015; Wu et al. 2014; Linford et al. 2011). Doppler factor δ can directly measure the significance of the jet beaming effect; a reliable determination of the Doppler factor, δ, is a key step in studying the physical process associated with the compact emission regions of AGNs (e.g., Wu et al. 2007). However, the Doppler factor calculation is quite difficult and there is no reliable method that can be applied to all the sources (e.g., Wu et al. 2007). According to the beaming model of AGNs, the emissions are composed of two parts, which are a boosted core and isotropic extended structures (e.g., Fan & Zhang 2003). The $R_{\rm CD}$ is calculated by using the ratio of two parts, $R_{\rm CD} = F_{\rm C}/F_{\rm E}$, where $F_{\rm C}$ and $F_{\rm E}$

are the fluxes of the boosted core and extended structure respectively (e.g., Orr & Browne 1982). On account of the jet emissions being very strongly beamed, the $R_{\rm CD}$ should reflect the orientation of the jet (e.g., Fan & Zhang 2003). To some extent, the $R_{\rm CD}$ is associated with the beaming effect in AGNs (e.g., Fan et al. 2011). Fan et al. (2006) found a significant correlation between the $R_{\rm CD}$ and the Doppler factor δ derived from the lowest γ-ray flux. It will be effective for us to use $R_{\rm CD}$ instead of the Doppler factor to investigate the relation between beaming and γ-ray detection for our sources in this work.

Although it is believed that beaming is an important parameter for the detection of γ-ray flux, the roles played by other parameters are still unclear. Wu et al. (2014) demonstrated that the Doppler factor is an important parameter for γ-ray detection. The non-detection of γ-ray emission in BL Lacs is likely due to the low beaming effect and/or low intrinsic γ-ray flux. One important aim of this paper is to test whether this property is still valid for the γ-ray detection of other types of AGNs.

This paper is organized as follows: the sample selection is described in Section 2; the results are shown in Section 3; the discussion is presented in Section 4; and the summary is given in Section 5. Throughout the paper we define the spectral index α as $f_\nu \propto \nu^{-\alpha}$, where f_ν is the flux density at frequency ν, and a cosmology with $H_0 = 70\,{\rm km\,s^{-1}\,Mpc^{-1}}$, $\Omega_{\rm M} = 0.3$ and $\Omega_\Lambda = 0.7$ is used. All values of luminosity applied in this paper are calculated with our adopted cosmological parameters.

2 THE SAMPLE

Fan & Zhang (2003) present a large sample of 542 extragalactic radio sources (27 BL Lacs, 215 quasars and 300 galaxies) that include $R_{\rm CD}$ at 5 GHz and other parameters. Under the assumption that the core spectral index is $\alpha_{\rm C} = 0.0$ and the extended spectral index can be $\alpha_{\rm E} = 0.5$ or 1.0, $R_{\rm CD}$ is derived as $R_{\rm CD} = \frac{L_{\rm C}}{L_{\rm E}} = \frac{L_{\rm C}}{L_{\rm T}-L_{\rm C}}(1.4/5)^{-\alpha_{\rm E}}(1+z)^{-\alpha_{\rm E}}$, where $L_{\rm C}$ is the 5 GHz radio core luminosity, $L_{\rm E}$ is the 5 GHz extended luminosity and $L_{\rm T}$ is the 1.4 GHz total luminosity (see Fan & Zhang 2003 for details).

In this work, we cross-correlate this sample with the 3FGL (Acero et al. 2015). This offers a sample of 80 γ-ray detected AGNs, including 22 BL Lac objects, 11 radio galaxies, 3 Seyfert galaxies and 44 quasars (see Table 1).

The energy range of γ-ray flux and luminosity is from 100 MeV to 300 GeV. The corresponding results are listed in Table 1, in which Col.1 is the source name, Col.2 is identification (BL stands for BL Lac object, Q for quasar, G for radio galaxy, and S, S1 and S2 for Seyfert galaxy), Col.3 is redshift, Col.4 is total luminosity at 1.4 GHz, Col.5 is core luminosity at 5 GHz, Col.6 and Col.7 are $R_{\rm CD}$ corresponding to $\alpha_{\rm E} = 0.5$ and 1.0 respectively, and Col.8 is γ-ray luminosity. In total, we have a sample of 542 extragalactic sources containing 80 *Fermi* objects (22 BL Lacs, 44 quasars and 14 galaxies) and 462 non-*Fermi* objects (5 BL Lacs, 171 quasars and 286 galaxies).

3 THE RESULTS

To study the differences between FAGNs and NFAGNs, we compare various radio properties for two subsamples, including $R_{\rm CD}$ and the core and extended luminosity. The results are shown as follows.

3.1 The Distributions of $R_{\rm CD}$ for FAGNs and NFAGNs

Figure 1 shows the $R_{\rm CD}$ distribution of FAGNs and NFAGNs with different extended spectral indexes, $\alpha_{\rm E}$ (with both $\alpha_{\rm E} = 0.5$ and $\alpha_{\rm E} = 1.0$). Through the comparison, we can learn that the distribution of $R_{\rm CD}$ from different values of extended spectral index $\alpha_{\rm E}$ is similar for both FAGNs and NFAGNs. Because of their similarity, we only adopt $\alpha_{\rm E} = 1.0$ for the rest of our results. From Figure 1, we can also find that the $R_{\rm CD}$ values of NFAGNs are on average smaller than those of FAGNs for both cases of $\alpha_{\rm E}$. Using the Kolmogorov-Smirnov (KS) test, we find that the $R_{\rm CD}$ distributions between FAGNs and NFAGNs are significantly different (with chance probability P $\sim 10^{-17}$). The mean values for FAGNs and NFAGNs are $\log R_{\rm CD} = 0.13$ and $\log R_{\rm CD} = -0.86$ respectively.

The distributions of $R_{\rm CD}$ for quasars and radio galaxies are shown in Figure 2. Through the KS test, we find that the $R_{\rm CD}$ distributions of *Fermi* quasars and non-*Fermi* quasars are significantly different (with chance probability $P \sim 10^{-7}$). The mean values are $\log R_{\rm CD} = 0.40$ and $\log R_{\rm CD} = -0.43$ respectively. However, considering the *Fermi* galaxies versus non-*Fermi* galaxies, the result of the KS test shows that there is no significant difference ($P = 0.713$), although the mean value of $R_{\rm CD}$ for *Fermi* galaxies ($\log R_{\rm CD} = -0.89$) is also higher than the value for non-*Fermi* galaxies ($\log R_{\rm CD} = -1.14$). Because the number of *Fermi* galaxies is very small, only 14 among the 300 galaxies, this result might not be a general conclusion. Additionally, because the majority of BL Lacs (22 of 27) in this sample are detected by *Fermi*, the difference between FBL and NFBLs is not studied in this work. The corresponding results for BL Lacs can be referred to in Wu et al. (2014).

3.2 The Radio Emission of FAGNs and NFAGNs

In this part, we study the difference in radio core luminosity for *Fermi* and non-*Fermi* sources as shown in Figure 3. It shows a tendency that the sources detected with *Fermi* have on average higher core-luminosity than sources not detected. From the KS test, the distributions of core luminosity between FAGNs and NFAGNs are significantly different ($P \sim 10^{-9}$ for all, $P \sim 10^{-5}$ for quasars only). However for galaxies, the result of the KS test shows that they do not have significant differences ($P = 0.458$), but the mean values for *Fermi*-galaxies ($\log L_{\rm C} = 23.29$) are slightly higher than the value for non-*Fermi* galaxies ($\log L_{\rm C} = 23.15$).

The relations between $R_{\rm CD}$ and $\log L_{\rm C}$, and between $R_{\rm CD}$ and $\log L_E$, are all studied and shown in Figure 4.

Table 1 The Various Parameters Associated with γ-ray Detected Sources from Fan & Zhang (2003)

Name	ID	z	$\log L_{\rm T}$ (W Hz^{-1})	$\log L_{\rm C}$ (W Hz^{-1})	$\log R_{\rm CD}$ $\alpha_{\rm E}=0.5$	$\log R_{\rm CD}$ $\alpha_{\rm E}=1.0$	L_γ (erg s^{-1})
(1)	(2)	(3)	(4)	(5)	(6)	(7)	(8)
0414+009	BL	0.287	25.30	24.70	−0.20	0.08	45.33
0521–365	BL	0.061	25.83	24.75	−0.77	−0.49	44.74
0548–322	BL	0.069	24.39	23.60	−0.44	−0.16	43.66
0723–008	BL	0.130	25.99	24.89	−0.79	−0.51	44.25
0828+493	BL	0.548	26.73	25.90	−0.48	−0.21	45.51
0829+046	BL	0.180	25.55	25.35	0.51	0.79	45.47
0954+658	BL	0.386	26.28	25.48	−0.45	−0.17	45.97
1011+496	BL	0.200	25.25	24.91	0.20	0.48	46.01
1101+384	BL	0.031	23.68	23.47	0.48	0.76	44.93
1156+295	BL	0.729	27.10	26.99	0.82	1.09	47.30
1219+285	BL	0.100	25.56	24.26	−1.00	−0.72	45.07
1413+135	BL	0.249	25.91	25.61	0.28	0.55	45.11
1652+398	BL	0.034	24.30	23.69	−0.21	0.07	44.54
1749+096	BL	0.322	26.16	25.83	0.22	0.50	46.12
1749+701	BL	0.770	27.57	26.52	−0.73	−0.46	47.10
1803+784	BL	0.680	27.34	26.97	0.15	0.42	47.08
1807+698	BL	0.050	24.84	24.60	0.41	0.68	44.36
1826+796	BL	0.664	27.39	26.88	−0.07	0.20	46.73
2131–021	BL	0.557	26.87	26.82	1.19	1.47	46.21
2200+420	BL	0.069	25.77	25.07	−0.33	−0.05	45.31
2201+044	BL	0.028	24.10	23.41	−0.31	−0.04	42.99
2240–260	BL	0.774	26.87	26.73	0.70	0.97	46.74
0305+039	G	0.029	24.83	23.77	−0.74	−0.47	43.11
0518–458	G	0.034	25.93	24.01	−1.64	−1.36	43.10
0755+379	G	0.041	24.49	23.59	−0.57	−0.29	43.05
0909+162	G	0.085	24.17	21.99	−1.90	−1.62	43.79
1010+350	G	1.414	27.14	26.87	0.34	0.62	46.91
1253–055	G	0.014	24.23	22.13	−1.82	−1.54	44.02
1322–427	G	0.001	24.62	22.12	−2.22	−1.95	41.16
1343–601	G	0.012	25.20	23.58	−1.33	−1.06	42.91
1441+522	G	0.140	25.05	23.44	−1.32	−1.05	44.06
1641+399	G	0.110	24.93	23.21	−1.44	−1.16	45.04
1823+568	G	0.088	24.84	23.65	−0.88	−0.61	44.74
1142+198	S	0.021	24.48	23.09	−1.10	−0.82	42.47
0240–002	S1	0.004	22.94	20.99	−1.67	−1.39	41.39
1637+826	S2	0.023	24.14	23.66	−0.03	0.25	43.12
0202+149	Q	0.833	27.61	27.23	0.13	0.41	46.53
0212+735	Q	2.367	28.59	28.20	0.11	0.39	47.95
0333+321	Q	1.258	28.36	27.23	−0.82	−0.54	47.26
0420–014	Q	0.915	27.82	27.26	−0.14	0.13	47.40
0528+134	Q	2.070	28.62	27.97	−0.26	0.01	48.19
0605–085	Q	0.870	27.86	27.37	−0.04	0.23	47.00
0637–752	Q	0.654	27.84	27.40	0.03	0.31	46.58
0707+476	Q	1.310	27.81	27.30	−0.07	0.20	46.96
0745+241	Q	0.410	26.56	25.88	−0.30	−0.03	45.59
0748+126	Q	0.889	27.26	27.21	1.19	1.47	46.69
0836+710	Q	2.160	28.51	27.67	−0.50	−0.22	48.10
0838+133	Q	0.684	27.23	26.45	−0.42	−0.15	46.18
0859+470	Q	1.462	28.17	27.27	−0.57	−0.29	46.83
0953+254	Q	0.712	26.66	26.53	0.73	1.01	46.44
1015+359	Q	1.226	27.18	27.16	1.60	1.88	46.57
1020+400	Q	1.254	27.51	26.70	−0.46	−0.18	46.73
1150+497	Q	0.334	26.43	25.85	−0.17	0.11	46.03
1217+023	Q	0.240	25.68	25.33	0.18	0.46	46.21
1222+216	Q	0.435	26.64	26.19	0.02	0.29	47.29
1226+023	Q	0.158	27.14	26.92	0.46	0.73	46.09
1315+346	Q	1.050	26.98	26.76	0.46	0.73	46.39
1418+546	Q	1.440	28.27	27.01	−0.96	−0.68	47.18
1451–375	Q	0.314	26.36	26.24	0.77	1.05	45.51
1508–055	Q	1.180	28.32	26.88	−1.15	−0.87	47.33
1510–089	Q	0.361	26.41	26.40	1.91	2.19	47.34
1510–089	Q	2.100	28.76	28.19	−0.16	0.12	49.21
1514–241	Q	1.546	26.64	25.49	−0.84	−0.57	47.95
1532+016	Q	1.440	27.78	27.07	−0.34	−0.06	47.06
1611+343	Q	1.401	27.88	27.78	0.86	1.14	46.99
1622–297	Q	0.815	27.26	27.18	0.97	1.25	46.96

Table 1 — *Continued.*

Name (1)	ID (2)	z (3)	$\log L_{\rm T}$ (W Hz^{-1}) (4)	$\log L_{\rm C}$ (W Hz^{-1}) (5)	$\log R_{\rm CD}$ $\alpha_{\rm E}=0.5$ (6)	$\log R_{\rm CD}$ $\alpha_{\rm E}=1.0$ (7)	L_γ (erg s^{-1}) (8)
1624+416	Q	2.550	28.57	27.99	−0.17	0.11	47.50
1633+382	Q	1.814	28.19	28.01	0.57	0.84	48.50
1638+398	Q	1.666	27.66	27.54	0.77	1.05	47.82
1800+440	Q	0.663	26.56	26.04	−0.09	0.19	46.25
1828+487	Q	0.692	27.94	27.30	−0.25	0.03	46.61
1842+681	Q	0.475	26.54	26.29	0.39	0.66	45.56
1849+670	Q	0.657	26.93	26.52	0.08	0.36	46.96
2007+777	Q	0.589	26.65	25.81	−0.50	−0.22	46.47
2037+511	Q	1.686	28.41	28.18	0.43	0.71	47.60
2145+067	Q	0.990	28.19	27.84	0.18	0.46	47.69
2201+315	Q	0.298	26.25	26.18	1.03	1.31	45.33
2230+114	Q	1.037	28.04	27.68	0.17	0.44	47.62
2251+158	Q	0.859	28.10	28.03	1.03	1.31	48.65
2335–027	Q	1.072	27.39	26.63	−0.40	−0.12	47.06

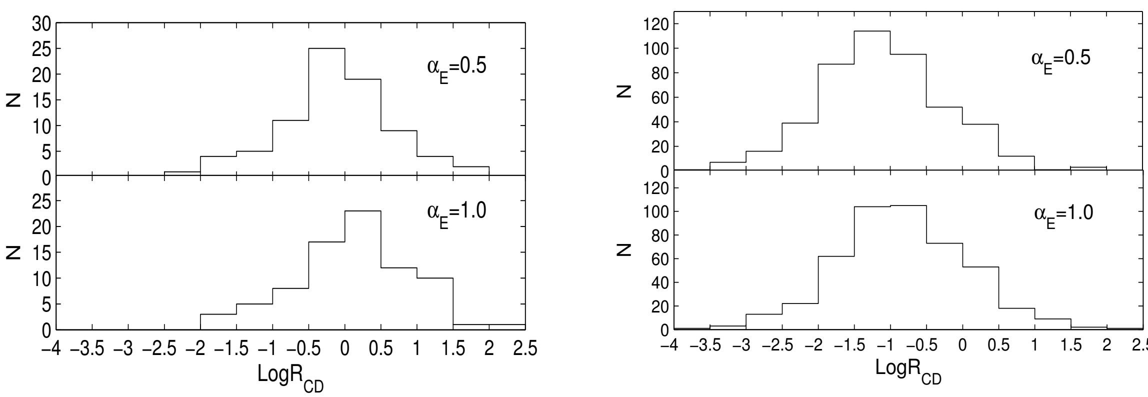

Fig. 1 Histograms of $\log R_{\rm CD}$ for FAGNs and NFAGNs with different values of extended spectral index $\alpha_{\rm E}$. The *left* and *right* panels show the cases for FAGNs and NFAGNs respectively. The *upper* panels correspond to $\alpha_{\rm E}=0.5$ and the *lower* panels to $\alpha_{\rm E}=1.0$.

We find there are positive correlations between $R_{\rm CD}$ and L_c for both FAGNs and NFAGNs, with correlation coefficients $r=0.49$ and 0.46 respectively, and all at a confidence level over 99.99% by Spearman rank correlation analysis. According to the beaming model of AGNs (Urry & Padovani 1995), the parameters $R_{\rm CD}$ and $L_{\rm C}$ both rely on Doppler factor δ, $R_{\rm CD}=R'_{\rm CD}\times\delta^2$ and $L_{\rm C}=L'_{\rm CD}\times\delta^2$ (assuming the spectral index $\alpha=0$), where $R'_{\rm CD}$ and $L'_{\rm CD}$ are intrinsic core dominance parameter and core luminosity respectively. Because radio galaxies are believed to be the parent population of blazars, Fan & Zhang (2003) and this work found that there is no correlation between $R_{\rm CD}$ and $L_{\rm C}$ for radio galaxies, which indicates that the $R'_{\rm CD}$ and $L'_{\rm CD}$ are probably not related. This suggests that the strong correlation between $R_{\rm CD}$ and $\log L_{\rm C}$ is probably because they both depend on δ, which means beaming plays an important role in the detected radio core flux and $R_{\rm CD}$ is a good indicator of the Doppler factor. This is consistent with the beaming model of AGNs (Urry & Padovani 1995). Moreover, for $R_{\rm CD}$ and $L_{\rm E}$, there is no significant correlation; we also found there are no significant differences for the distribution of $L_{\rm E}$ between *Fermi*-QSOs and non-*Fermi*-QSOs, and between *Fermi*-galaxies and non-*Fermi* galaxies, which indicate that the extended luminosity is less influenced by the beaming effect.

Because δ is an important parameter for the detection of radio flux, the systematically higher mean and median radio core luminosity in FAGNs indicates that the γ-ray detection of FAGNs might be caused by their higher beaming effect, but we cannot exclude the possibility that their intrinsic flux might also play a role.

3.3 The γ-ray Emission and $R_{\rm CD}$

We have obtained the γ-ray flux in the 100 MeV to 300 GeV energy range for 80 sources in Fan & Zhang (2003) from the 3FGL and calculated the γ-ray luminosity. We found a strong correlation between $R_{\rm CD}$ and L_γ, with a correlation coefficient of $r=0.39$ at the $>99.9\%$ confidence level, which is shown in the left panel of Figure 5. In addition, we also consider the correlation between $R_{\rm CD}$ and γ-ray flux F_γ, which is shown in the right panel of Figure 5, with a correlation coefficient of $r=0.28$ at the $>98\%$ confidence level. Because $R_{\rm CD}=R'_{\rm CD}\times\delta^2$, these

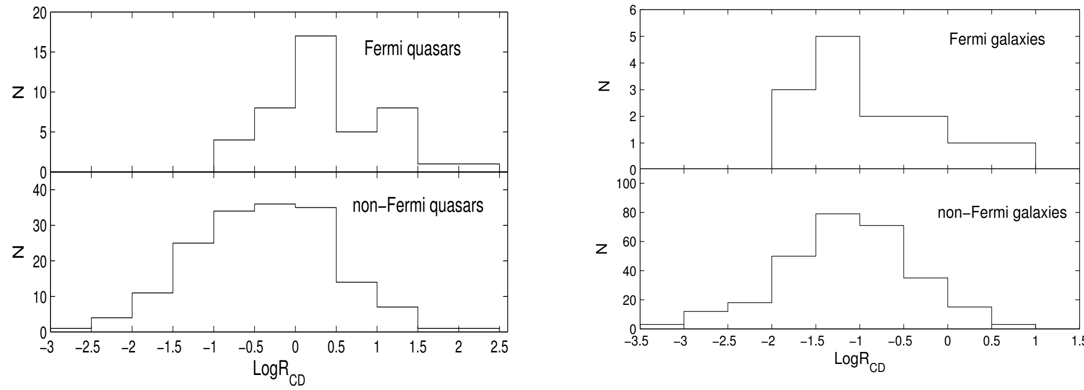

Fig. 2 Histograms showing the comparison of $R_{\rm CD}$ for quasars (*right*) and galaxies (*left*) (*upper* panels are for *Fermi* sources and *lower* panels are for non-*Fermi* sources).

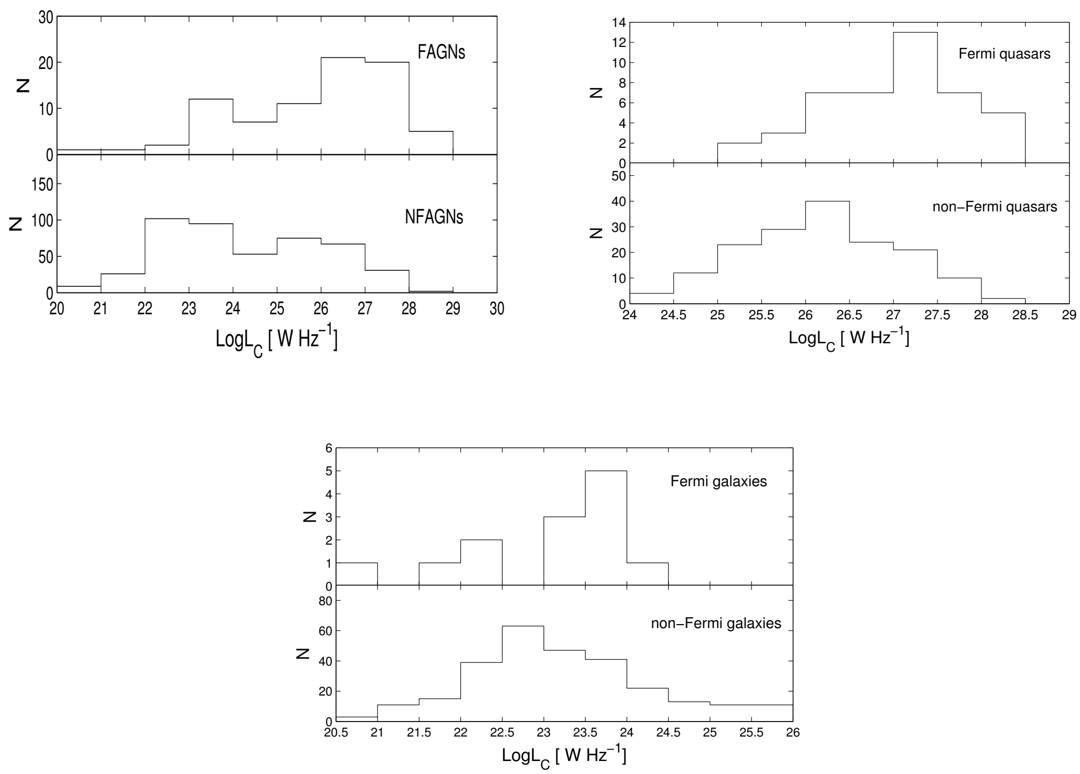

Fig. 3 Comparisons of the core luminosity for complete samples (*upper left*), quasars (*upper right*) and galaxies (*lower*).

correlations might be caused by the parameters ($R_{\rm CD}$, L_γ and F_γ) all depending on the Doppler factor δ. These results indicate that γ-ray emission is probably influenced by the jet beaming effect, and $R_{\rm CD}$ can be treated as an indicator of the beaming effect.

4 DISCUSSION

In this work, based on a large sample of radio sources with $R_{\rm CD}$ (e.g., Fan & Zhang 2003), we found significant differences in $R_{\rm CD}$ for FAGNs and NFAGNs, as well as for *Fermi* quasars and non-*Fermi* quasars. There is a tendency that the *Fermi* sources have on average higher $R_{\rm CD}$ than the non-*Fermi* sources. The radio core luminosity of FAGNs is also systematically higher than that of NFAGNs. These results suggest that *Fermi* sources probably exhibit a strong beaming effect, consistent with results in the literature (e.g. Wu et al. 2014; Chen et al. 2015) and imply that $R_{\rm CD}$ is probably an indicator of the jet beaming effect and that it plays an important role in the γ-ray detection among AGNs in this present sample.

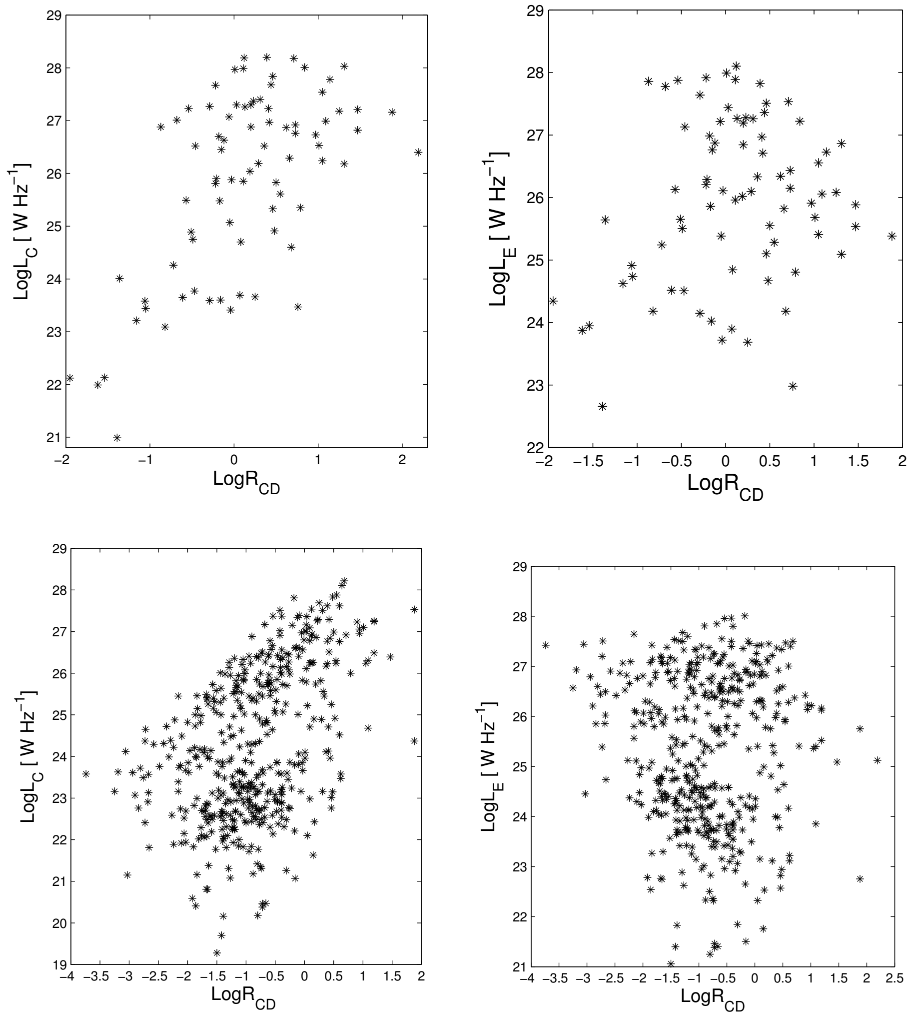

Fig. 4 Relations between $R_{\rm CD}$ and core (*left*) and extended (*right*) luminosities for both FAGNs and NFAGNs (the *top* two panels are correlations for FAGNs; the *bottom* two panels are for NFAGNs).

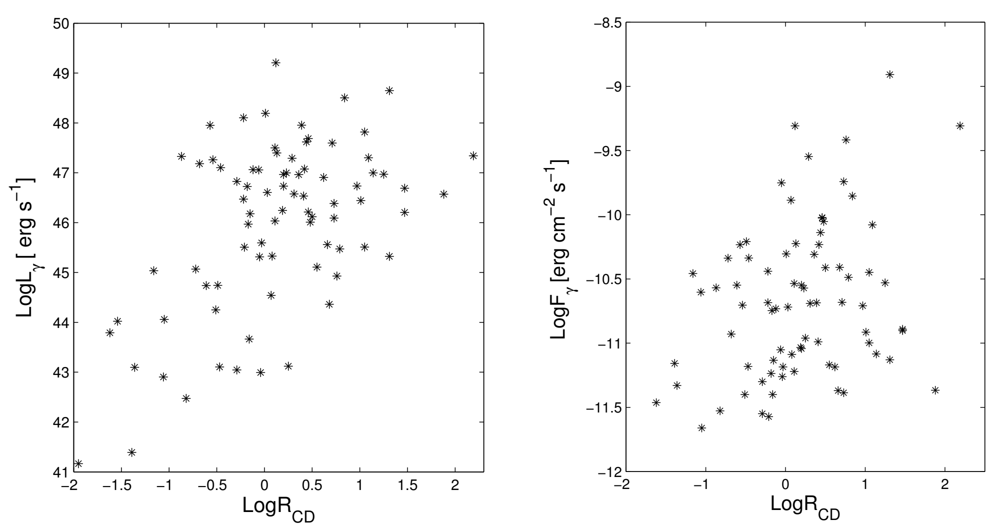

Fig. 5 The *left* panel is the relation between $\log R_{\rm CD}$ and $\log L_{\gamma}$, and the *right* panel is that between $\log R_{\rm CD}$ and F_{γ}.

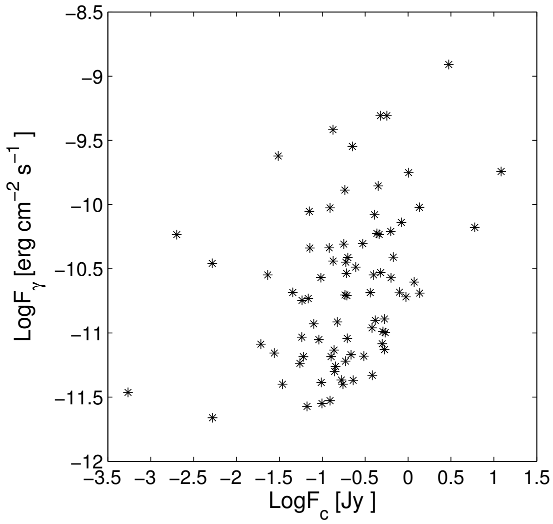

Fig. 6 The relation between radio core flux at 5 GHz and γ-ray flux in the 100 MeV to 100 GeV range.

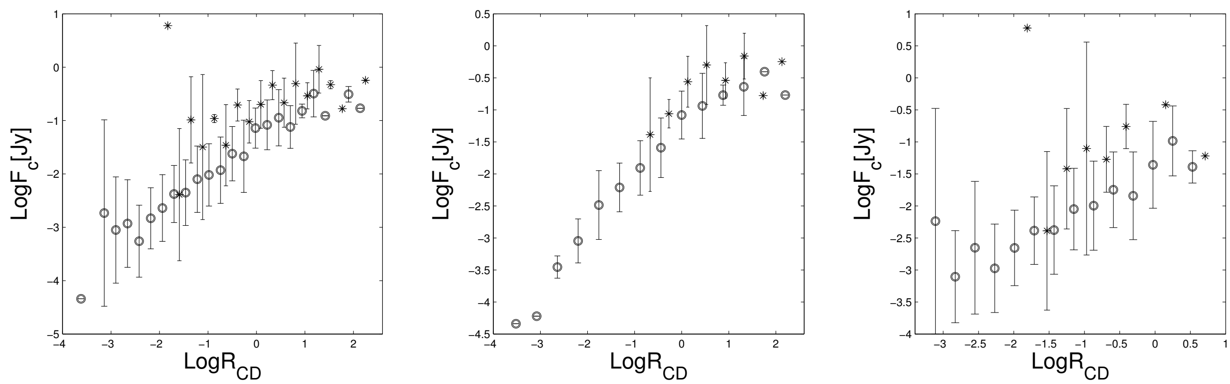

Fig. 7 The correlation between $R_{\rm CD}$ and the radio core flux, in which errorbars show the standard deviation of core flux. The asterisks represent FAGNs and the open circles represent NFAGNs. The *left*, *middle* and *right* panels show the cases for the complete sample, quasars and galaxies, respectively.

4.1 The Correlation between Radio Core Flux and γ-ray Emission

Ghirlanda et al. (2011), Ackermann et al. (2011) and Ackermann et al. (2015) all demonstrate that there is a statistically significant positive correlation between the centimeter radio and the γ-ray energy flux. Wu et al. (2014) show a significant correlation between γ-ray flux and radio core flux for a sample of BL Lac objects. A similar correlation is also found for our present sample, see Figure 6. Because γ-ray flux and radio core flux are Doppler boosted, a strong correlation between them is expected, after excluding the common dependence on $R_{\rm CD}$ which is an indicator of Doppler factor by using the partial Spearman correlation method with a correlation coefficient of 0.33 at a confidence level $> 99\%$. Considering the correlation between radio core flux F_c and γ-ray flux F_γ, NFAGNs may have both smaller F_c and smaller F_γ, even though they have comparable $R_{\rm CD}$ with FAGNs, which makes them more difficult to be detected by *Fermi*-LAT.

4.2 Why are Some Sources Detected with *Fermi* but Others are Not?

Wu et al. (2014) indicate that the Doppler factor is an important parameter for γ-ray detection. The non-detection of γ-ray emission in NFBLs is likely due to a low beaming effect, and/or low intrinsic γ-ray flux. The one important aim of this paper is to test if the results for the BL Lac sample in Wu et al. (2014) are still valid for other types of AGN samples. We studied the differences of FAGNs and NFAGNs through radio core flux at fixed $R_{\rm CD}$.

In Figure 7, we show the correlation between $R_{\rm CD}$ and the average F_c of FAGNs and NFAGNs in $R_{\rm CD}$ bins, similar to Wu et al. (2014). The panels from left to right display the cases for the complete sample, quasars and galaxies, respectively (with corresponding bin sizes of 0.24, 0.4 and 0.28 for $\log R_{\rm CD}$). From these panels, we can see that FAGNs have systematically larger radio core flux than NFAGNs at fixed $R_{\rm CD}$, indicating larger intrinsic radio core flux in FAGNs. This result is consistent with the result of BL Lac objects in Wu et al. (2014).

Because FAGNs have systematically larger radio core flux than NFAGNs at fixed $R_{\rm CD}$, their extended flux is also expected to be larger. Considering the strong linear correlation between intrinsic radio core emission and extended emission (Giovannini et al. 2001), the extended flux for FAGNs should also be larger than that of NFAGNs because of their systematically larger radio core flux, but no strong correlations are found between extended emission and γ-ray emission for this sample. This may be caused by our sample being small and the result indicates that the intrinsic emission is one possible factor but might not be the crucial factor for the detection of γ-ray emission as the Doppler factor. Further study of a larger sample of γ-ray AGNs might find the correlations between extended radio emission and γ-ray emission and test our predications.

Together with the results in Wu et al. (2014), we can see that *Fermi* detected BL Lacs, QSOs and radio galaxies all have larger intrinsic radio core flux than their non-detected samples. These results indicate a strong connection between radio and γ-ray emission for the present sample, and it seems to favor the far-dissipation scenario presented by Ramakrishnan et al. (2015) and Nieppola et al. (2011): there is a co-spatial origin of the activity for the radio and γ-ray emission, suggesting that the origin of the seed photons for the high-energy γ-ray emission is within the jet.

5 SUMMARY

In this paper, we have compared the multiple parameters describing FAGNs and NFAGNs by using available data from the literature. We found that $R_{\rm CD}$ has clear correlations with core luminosity, γ-ray luminosity and γ-ray flux. The average $R_{\rm CD}$ in the *Fermi* sources is larger than that in the non-*Fermi* sources. Moreover, there is a tendency that the *Fermi* sources have higher core-luminosity than the non-*Fermi* sources for the complete sample, quasars and galaxies. We also show that FAGNs have systematically larger radio core flux than NFAGNs at fixed $R_{\rm CD}$, indicating larger intrinsic radio core flux in FAGNs.

Our results imply that $R_{\rm CD}$ plays an important role in the jet beaming effect used in γ-ray detection. They also show that the beaming effect is vital for the detection of γ-ray emission. The non-*Fermi* sources are likely due to the low beaming effect and/or the low intrinsic γ-ray flux. The strong connections between radio and γ-ray emission might suggest that the origin of the seed photons for the high-energy γ-ray emission is within the jet for this AGN sample.

On account of our sample being limited by the available archival data, a future larger sample of new observational data including redshift, radio core luminosity, extended luminosity and γ-ray luminosity will be used for further tests of our results.

Acknowledgements We thank an anonymous referee for insightful comments and constructive suggestions. This work is supported by the National Natural Science Foundation of China (Nos. U1431111, 11163002, 11473054 and U1531245) and by the Science and Technology Commission of Shanghai Municipality (Grant 14ZR1447100).

References

Acero, F., Ackermann, M., Ajello, M., et al. 2015, ApJS, 218, 23
Ackermann, M., Ajello, M., Allafort, A., et al. 2011, ApJ, 741, 30
Ackermann, M., Ajello, M., Atwood, W. B., et al. 2015, ApJ, 810, 14
Atwood, W. B., Abdo, A. A., Ackermann, M., et al. 2009, ApJ, 697, 1071
Chen, Y. Y., Zhang, X., Zhang, H. J., & Yu, X. L. 2015, MNRAS, 451, 4193
Fan, J.-H., Yang, J.-H., Pan, J., & Hua, T.-X. 2011, RAA (Research in Astronomy and Astrophysics), 11, 1413
Fan, J. H., & Zhang, J. S. 2003, A&A, 407, 899
Fan, Z., Cao, X., & Gu, M. 2006, ApJ, 646, 8
Ghirlanda, G., Ghisellini, G., Tavecchio, F., Foschini, L., & Bonnoli, G. 2011, MNRAS, 413, 852
Giovannini, G., Cotton, W. D., Feretti, L., Lara, L., & Venturi, T. 2001, ApJ, 552, 508
Linford, J. D., Taylor, G. B., Romani, R. W., et al. 2011, ApJ, 726, 16
Linford, J. D., Taylor, G. B., Romani, R. W., et al. 2012, ApJ, 744, 177
Lister, M. L., Aller, M. F., Aller, H. D., et al. 2015, ApJ, 810, L9
Nieppola, E., Tornikoski, M., Valtaoja, E., et al. 2011, A&A, 535, A69
Orr, M. J. L., & Browne, I. W. A. 1982, MNRAS, 200, 1067
Piner, B. G., Pushkarev, A. B., Kovalev, Y. Y., et al. 2012, ApJ, 758, 84
Pushkarev, A. B., & Kovalev, Y. Y. 2012, A&A, 544, A34
Ramakrishnan, V., Hovatta, T., Nieppola, E., et al. 2015, MNRAS, 452, 1280
Urry, C. M., & Padovani, P. 1995, PASP, 107, 803
Wu, Z., Jiang, D., Gu, M., & Chen, L. 2014, A&A, 562, A64
Wu, Z., Jiang, D. R., Gu, M., & Liu, Y. 2007, A&A, 466, 63
Xiong, D., Zhang, X., Bai, J., & Zhang, H. 2015, MNRAS, 451, 2750